An Extended Jacobian-Based Formulation for Operational Space Control of Kinematically Redundant Robot Manipulators With Multiple Subtask Objectives: An Adaptive Control Approach

Kamil Cetin
Department of Electrical & Electronics Engineering,
Izmir Institute of Technology,
Urla, Izmir 35430, Turkey
e-mail: kamilcetin@iyte.edu.tr

Enver Tatlicioglu[1]
Department of Electrical & Electronics Engineering,
Izmir Institute of Technology,
Urla, Izmir 35430, Turkey
e-mail: enver@iyte.edu.tr

Erkan Zergeroglu
Department of Computer Engineering,
Gebze Technical University,
Gebze, Kocaeli 41400, Turkey
e-mail: e.zerger@gtu.edu.tr

In this study, an extended Jacobian matrix formulation is proposed for the operational space tracking control of kinematically redundant robot manipulators with multiple subtask objectives. Furthermore, to compensate the structured uncertainties related to the robot dynamics, an adaptive operational space controller is designed, and then, the corresponding stability analysis is presented for kinematically redundant robot manipulators. Specifically, the proposed method is concerned with not only the stability of operational space objective but also the stability of multiple subtask objectives. The combined stability analysis of the operational space objective and the subtask objectives are obtained via Lyapunov based arguments. Experimental and simulation studies are presented to illustrate the performance of the proposed method. [DOI: 10.1115/1.4042464]

1 Introduction

Kinematically redundant robot manipulators have a greater number of joints than the number of variables necessary to describe a given task. Due to the differences between the dimension of the joint space (i.e., n) and the dimension of operational space (Cartesian space or end-effector space) (i.e., m) of kinematically redundant robot manipulators, there exist n–m redundant degree-of-freedom (DOF) [1], thus generating at least one independent parameter to define the output configuration to perform a desired task in the operational space. However, from a mathematical perspective, this redundancy exposes an inverse kinematic problem for kinematically redundant robot manipulators due to the infinite many joint configuration solutions for any given desired position of the end-effector. In spite of the inverse kinematic problem, taking the advantage of this redundancy while properly manipulating the kinematically redundant robot manipulator in the operational space, joint motion in the null-space of the Jacobian matrix can be used to perform subtasks (secondary objectives) such as special joint configurations, avoidance of singularities, manipulability enhancement, joint limit avoidance, and obstacle avoidance. For a more detailed review of the topic on kinematically redundant robot manipulators, the interested reader referred to Refs. [2]–[4] with their references. From a quick review of this topic in literature, researchers generally focused on two major redundancy resolution (inverse kinematic) methods for the aforementioned problem: (i) pseudo-inverse Jacobian-based control formulations and (ii) redundancy resolution via an extended Jacobian (task augmentation).

In early research on pseudo-inverse Jacobian-based control formulation for redundancy resolution, first, Khatib [5] proposed this formulation and developed a control method based on the dynamic model of a robot manipulator in operational space. Then, Hsu et al. [6] presented a feedback linearization controller that guarantees end-effector tracking and enables the self-motion of the manipulator flow along the projection of a given arbitrary vector field. To deal with simultaneous multiple objectives, recently, Ott et al. [7] proposed a null space projection-based approach for dynamic control of kinematically redundant robot manipulator. However, these control methods were based on exact knowledge of the robot dynamics. For the same problem with dynamical uncertainties, adaptive control methods were presented for kinematically redundant robot manipulators in Refs. [8]–[16]. To compensate unstructured uncertainties in robot dynamics, robust control methods were presented in Refs. [17]–[21]. Most of these pseudo-inverse Jacobian-based robust and adaptive control methods achieved end-effector tracking without the integration of the subtask objective into the stability analysis. First, in Refs. [11] and [12], the authors addressed this issue by designing an adaptive controller that achieved asymptotic tracking in the operational space in conjunction with systematic integration of the subtask objective into the stability analysis. Later, the proposed methodology of Ref. [16] ensured a combined stability analysis for both operational space tracking and subtask objectives. However, in Ref. [16], only one subtask objective can be performed since the proposed methodology was applicable for one redundant DOF (i.e., $n-m=1$). One of our motivations in this study arises from the requirement of multiple subtask objectives for highly redundant robot manipulators (i.e., $n-m>1$).

As noted in Ref. [4], the extended Jacobian methods have a major advantage over pseudo-inverse Jacobian-based methods in that it is cyclic (also called repeatability). It is mentioned that the motion of the robot manipulator during periodic tasks to be recurrently repeated may be unpredictable. In early research on the extended Jacobian method for redundancy resolution, in Ref. [22], Baillieul proposed this method that projects the gradient of the cost function onto the null space of the Jacobian. In another

[1]Corresponding author.

Contributed by the Dynamic Systems Division of ASME for publication in the Journal of Dynamic Systems, Measurement, and Control. Manuscript received February 23, 2018; final manuscript received December 22, 2018; published online January 29, 2019. Assoc. Editor: Soo Jeon.

augmentation method for solving kinematic redundancy [23], Seraji proposed an augmented inverse Jacobian for controlling the manipulator configuration. In Ref. [24], the authors proposed a steady motion control for redundant robot manipulators using an extended operational space formulation. Robust adaptive control for redundant manipulators, presented in Ref. [25], ensures the global stability of trajectory tracking objective in the presence of bounded disturbances. The authors in Ref. [26] used the extended Jacobian method of Ref. [22] for redundant robot manipulator control with obstacle avoidance. Simas et al. [27] proposed an extended Jacobian matrix based on kinematic constraints and applied for collision avoidance of a P3R redundant robot manipulator. For the problem of inverse Jacobian kinematics, the authors in Ref. [28] developed an extended Jacobian approximation algorithm combining the advantages of both the pseudo-inverse Jacobian method and the extended Jacobian method. However, all these methods mentioned above did not consider the stability analysis of subtask objectives.

In this study, we propose an extended Jacobian based adaptive operational space controller formulation that makes use of subtask objectives to extend the manipulator Jacobian. The use of subtask objectives to extend the manipulator Jacobian enables the proposed controller to perform both the main end-effector tracking objective and an extra subtask objective at the same time. Specifically, an extended operational space formulation is designed by integrating the null-space of the Jacobian matrix with the operational space Jacobian matrix. Additional subtask functions depending on the joint motion with equality constraints are properly chosen up to the amount of the redundant DOF. In order to compensate for parametric uncertainties in the robot dynamics, an adaptive controller is designed. A Lyapunov stability theorem is then proposed, and asymptotic stability of the designed controller is ensured. This study presents a major improvement to the literature in the sense that multiple subtask objectives can be performed along with the main operational space objective. In addition, the performance of the proposed extended operational space formulation is experimentally validated using a 3DOF kinematically redundant robot manipulator, and then, a simulation study is performed on the model of 4DOF manipulator on MATLAB/SIMULINK. For the subtask objectives, inspired from Ref. [29], we developed a function which aims that a fixed laser or optic camera on the first joint accurately tracks the end-effector of the manipulator.

The rest of this paper is organized as follows: dynamic and kinematic models for robot manipulator are given in Sec. 2. Extended operational space formulation is provided in Sec. 3. Error system formulation is provided in Sec. 4. Section 5 presents the design and the stability analysis of the adaptive operational space controller. The experimental and simulation results are given in Secs. 6 and 7, respectively, and concluding remarks are given in Sec. 8.

2 Dynamic and Kinematic Models

The dynamic model of an n DOF revolute joint robot manipulator is described as [6]

$$M(\theta)\ddot{\theta} + V_m(\theta,\dot{\theta})\dot{\theta} + G(\theta) + F_d\dot{\theta} = \tau(t) \tag{1}$$

where $\theta(t), \dot{\theta}(t), \ddot{\theta}(t) \in \mathbb{R}^n$ are the joint position, velocity, and acceleration vectors, respectively, $M(\theta) \in \mathbb{R}^{n\times n}$ represents the mass-inertia matrix, $V_m(\theta,\dot{\theta}) \in \mathbb{R}^{n\times n}$ represents centripetal-Coriolis effects, $G(\theta) \in \mathbb{R}^n$ represents gravitational effects, $F_d \in \mathbb{R}^{n\times n}$ is the constant, diagonal, positive definite dynamic frictional effects, and the control input torque vector is defined as $\tau(t) \in \mathbb{R}^n$. For the development of controller and the stability analysis, the following properties are required [30].

PROPERTY 1. *The mass-inertia matrix $M(\theta)$ is symmetric and positive-definite and satisfies the following inequalities:*

$$m_1||\zeta||^2 \le \zeta^T M(\theta)\zeta \le m_2||\zeta||^2 \,\forall \zeta \in \mathbb{R}^n \tag{2}$$

where m_1, $m_2 \in \mathbb{R}$ are positive constants and $\|\cdot\|$ denotes the standard Euclidean norm.

PROPERTY 2. *The mass-inertia and centripetal-Coriolis matrices satisfy the following skew symmetric relationship:*

$$\zeta^T\left[\dot{M}(\theta) - 2V_m(\theta,\dot{\theta})\right]\zeta = 0 \,\forall \zeta \in \mathbb{R}^n \tag{3}$$

where $\dot{M}(\theta)$ denotes the time derivative of the mass-inertia matrix.

PROPERTY 3. *The left-hand side of (1) can be linearly parameterized as shown below*

$$Y(\theta,\dot{\theta},\ddot{\theta})\phi = M(\theta)\ddot{\theta} + V_m(\theta,\dot{\theta})\dot{\theta} + G(\theta) + F_d\dot{\theta} \tag{4}$$

where $Y(\theta,\dot{\theta},\ddot{\theta}) \in \mathbb{R}^{n\times p}$ is the regression matrix and $\phi \in \mathbb{R}^p$ is the constant parameter vector that depends on robot parameters.

The end-effector pose in the operational space $x(t) \in \mathbb{R}^m$ (with $n > m$) can be written as a function of the joint position as shown below

$$x = f(\theta) \tag{5}$$

where $f : \mathbb{R}^n \to \mathbb{R}^m$ is the forward kinematics function. Differentiating Eq. (5) with respect to time, the velocity kinematics can be written as

$$\dot{x} = J\dot{\theta} \tag{6}$$

where $\dot{x}(t) \in \mathbb{R}^m$ is the operational space velocity vector and $J(\theta) \triangleq \left(\partial f(\theta)/\partial\theta\right) \in \mathbb{R}^{m\times n}$ is the Jacobian matrix.

Following remarks are standard in the dynamic redundant robot control literature [5,30].

Remark 1. During the control development, we need $J(\theta)$ to be full-rank $\forall\theta$ which is possible by avoiding all kinematic singularities a priori.

Remark 2. The dynamic and kinematic terms of revolute joints robot manipulators depend on $\theta(t)$ via trigonometric functions only, and as result of this, they remain bounded for all possible $\theta(t)$.

3 Extended Operational Space Formulation

The subtask function, denoted by $y_s(\theta) \in \mathbb{R}^{(n-m)}$, will be specifically designed to depend only on θ as follows:

$$y_s = f_s(\theta(t)) \tag{7}$$

where $f_s : \mathbb{R}^n \to \mathbb{R}^{(n-m)}$. The time derivative of y_s can then be obtained as

$$\dot{y}_s = J_s\dot{\theta} \tag{8}$$

where $J_s(\theta) \in \mathbb{R}^{(n-m)\times n}$ is the subtask Jacobian defined as

$$J_s \triangleq \frac{\partial y_s}{\partial\theta} \tag{9}$$

In order to avoid utilizing pseudo inverse of the Jacobian matrix, we combine the m dimensional forward kinematics and the $(n-m)$ dimensional subtask objectives into $\bar{x}(t) \in \mathbb{R}^n$ defined as follows:

$$\bar{x}(t) \triangleq \begin{bmatrix} x \\ y_s \end{bmatrix} = \begin{bmatrix} f(\theta) \\ f_s(\theta) \end{bmatrix} \tag{10}$$

Taking the time derivative of Eq. (10) yields

$$\dot{\bar{x}} = \bar{J}\dot{\theta} \tag{11}$$

where $\bar{J}(\theta) \in \mathbb{R}^{n\times n}$ is the extended Jacobian matrix defined as

$$\bar{J} \triangleq \begin{bmatrix} J \\ J_s \end{bmatrix} \tag{12}$$

Remark 3. The extended Jacobian matrix $\bar{J}$ has full rank if and only if the subtask function $y_s(t)$ is carefully defined in terms of the joint positions θ.

The design objective is to make the end-effector position, $x(t)$, go to some desired position $x_d(t) \in \mathbb{R}^m$ and make subtask function, y_s, go to some desired subtask $y_d(t) \in \mathbb{R}^{(n-m)}$. Therefore, we define an extended desired position, denoted by $\bar{x}_d(t) \in \mathbb{R}^n$, as follows:

$$\bar{x}_d \triangleq \begin{bmatrix} x_d \\ y_d \end{bmatrix} \tag{13}$$

Remark 4. It is assumed that the extended desired positions with first-order and second-order time derivatives ($\bar{x}_d(t)$, $\dot{\bar{x}}_d(t)$, and $\ddot{\bar{x}}_d(t)$) are all bounded functions of time.

4 Error System Development

The tracking error, denoted by $e(t) \in \mathbb{R}^n$, is defined as follows:

$$e \triangleq \bar{x}_d - \bar{x} \tag{14}$$

By using the first-order time derivative of Eq. (14) and substituting Eq. (11), we obtain

$$\dot{e} = \dot{\bar{x}}_d - \bar{J}\dot{\theta} \tag{15}$$

To further simplify the stability analysis, we define an auxiliary error-like term, expressed by $r(t) \in \mathbb{R}^n$, as

$$r \triangleq \bar{J}^{-1}(\dot{\bar{x}}_d + \alpha e) - \dot{\theta} \tag{16}$$

where $\alpha \in \mathbb{R}^{n\times n}$ is a constant, diagonal, positive-definite control gain matrix. It is highlighted that in view of Remarks 1 and 3, inverse of the extended Jacobian matrix $\bar{J}^{-1}$ exists $\forall\theta$. Premultiplying Eq. (16) by $\bar{J}$ and substituting Eqs. (11) and (15), we obtain

$$\dot{e} = -\alpha e + \bar{J}r \tag{17}$$

By using the first-order time derivative of Eq. (16), premultiplying by mass-inertia matrix $M(\theta)$, and then substituting Eq. (1), we obtain the following open-loop error dynamics:

$$M\dot{r} = \bar{Y}\phi - V_m r - \tau \tag{18}$$

where

$$\bar{Y}\phi = M\frac{d}{dt}\{\bar{J}^{-1}(\dot{\bar{x}}_d + \alpha e)\} + V_m\bar{J}^{-1}(\dot{\bar{x}}_d + \alpha e) + G + F_d\dot{\theta} \tag{19}$$

with $\bar{Y}\left(\theta, \dot{\theta}, \bar{x}_d, \dot{\bar{x}}_d, \ddot{\bar{x}}_d, t, e, \dot{e}\right) \in \mathbb{R}^{n\times p}$ denoting an available regression matrix and $\phi \in \mathbb{R}^p$ representing the constant parameter vector (e.g., mass, inertia, and friction coefficients).

5 Adaptive Controller Design and Stability Analysis

In this section, the control design and the accompanying stability analysis will be presented. An adaptive control method is developed when parametric uncertainties exist in the dynamic model (i.e., the parameter vector ϕ in Eq. (19) is uncertain) provided full-state feedback.

Considering the error system formulations in Sec. 4, the following stability analysis and the compensation of uncertain dynamic model parameters, we design the control input torque $\tau(t)$ as

$$\tau = \bar{Y}\hat{\phi} + K_r r + \bar{J}^T e \tag{20}$$

where $K_r \in \mathbb{R}^{n\times n}$ is a positive-definite, constant, diagonal, control gain matrix and $\hat{\phi}(t) \in \mathbb{R}^p$ is the estimation of the uncertain parameter vector ϕ, and is updated according to

$$\dot{\hat{\phi}} = \Gamma\bar{Y}^T r \tag{21}$$

where $\Gamma \in \mathbb{R}^{p\times p}$ is a constant, positive definite, diagonal adaptive gain matrix. As can be seen from Eq. (20), pseudo-inverse Jacobian is not used in the controller. The parameter estimation error $\tilde{\phi}(t) \in \mathbb{R}^p$ is defined as

$$\tilde{\phi} \triangleq \phi - \hat{\phi} \tag{22}$$

Substituting Eqs. (20) and (22) into Eq. (18), the closed-loop error system for $r(t)$ can be written as follows:

$$M\dot{r} = -V_m r - K_r r - \bar{J}^T e + \bar{Y}\tilde{\phi} \tag{23}$$

Now the stability analysis can be easily proceeded for the adaptive controller. We begin our analysis by introducing the following Theorem:

THEOREM 1. *For the robot manipulator dynamics given in Eq. (1), the proposed adaptive controller in Eq. (20) with the estimation law of the uncertain parameter vector in Eq. (21) guarantees asymptotic operational space tracking and asymptotic subtask control in the sense that*

$$\|e(t)\| \to 0 \text{ as } t \to \infty \tag{24}$$

Proof. In order to prove Theorem 1, first, a non-negative scalar function (i.e., a Lyapunov function candidate), denoted by $V\left(e, r, \tilde{\phi}\right) \in \mathbb{R}$, is defined as

$$V \triangleq \frac{1}{2}e^T e + \frac{1}{2}r^T M r + \frac{1}{2}\tilde{\phi}^T\Gamma^{-1}\tilde{\phi}. \tag{25}$$

From the dynamic model Property 1, it can easily be observed that the following boundedness can be written for Eq. (25) as

$$\lambda_1||z||^2 \le V \le \lambda_2||z||^2 \tag{26}$$

where $\lambda_1 \triangleq (1/2)\min\{1, m_1, \lambda_{\min}(\Gamma)\}$, $\lambda_2 \triangleq (1/2)\max\{1, m_2, \lambda_{\min}(\Gamma)\}$ with $\lambda_{\max}(\cdot)$ and $\lambda_{\min}(\cdot)$ denoting the maximum and minimum eigenvalues of a matrix, respectively, and $z(t) \in \mathbb{R}^{(2n+p)}$ is the combined error-like vector defined as

$$z(t) \triangleq \begin{bmatrix} e^T & r^T & \tilde{\phi}^T \end{bmatrix}^{\mathrm{T}} \tag{27}$$

We can write the first-order time derivative of Eq. (25) as follows:

$$\dot{V} = e^T\dot{e} + r^T M\dot{r} + \frac{1}{2}r^T\dot{M}r + \tilde{\phi}^T\Gamma^{-1}\dot{\tilde{\phi}} \tag{28}$$

Substituting Eqs. (17), (23), and time derivative of Eq. (22) along with Eq. (21) into Eq. (28), and then canceling common terms with mathematical simplifications, we obtain the following equation:

$$\dot{V} = -e^T\alpha e - r^T K_r r \tag{29}$$

where Eq. (3) was also utilized. From a mathematical perspective, the right-hand side of Eq. (29) can be upper bound as

$$\dot{V} \le -\lambda_3\left(||e||^2 + ||r||^2\right) \tag{30}$$

where $\lambda_3 \triangleq \min\{\lambda_{\min}(\alpha), \lambda_{\min}(K_r)\}$.

From Eqs. (25), (26) and (29), (30), it is simple to observe that the defined nonscalar function $V(e, r, \tilde{\phi}) \in \mathcal{L}_\infty$, and therefore, the entries of the combined error vector $e(t)$, $r(t)$ and $\tilde{\phi}(t) \in \mathcal{L}_\infty$. From the boundedness of $\tilde{\phi}$ with Eq. (22), it is clear that $\hat{\phi}(t) \in \mathcal{L}_\infty$. Based on the boundedness of $\bar{x}_d(t)$, from Eq. (14), it is observed that $\bar{x}(t) \in \mathcal{L}_\infty$. In view of Remarks 2 and 4, boundedness of error terms $e(t)$ and $r(t)$ can be used along with Eq. (17) to conclude that $\dot{\bar{x}}(t) \in \mathcal{L}_\infty$. Above boundedness expression can be used with Eq. (16) to prove that $\dot{\theta}(t) \in \mathcal{L}_\infty$. In view of Remark 2, the boundedness of $\dot{\theta}$ can be used to prove that $V_m(\theta, \dot{\theta}) \in \mathcal{L}_\infty$. All boundedness expressions mentioned above can be used with Eq. (18) to prove that $\dot{r}(t) \in \mathcal{L}_\infty$. The robot manipulator dynamics in Eq. (1) can be used to demonstrate $\tau(t) \in \mathcal{L}_\infty$, and then, standard signal chasing arguments can be employed to prove that all signals remain bounded under the closed-loop operation. After integrating Eq. (30) in time from 0 to $+\infty$, we obtain

$$\int_0^{+\infty} \dot{V}(t)dt \leq -\lambda_3 \int_0^{+\infty} \left(||e(t)||^2 + ||r(t)||^2\right)dt \tag{31}$$

and after some mathematical manipulations

$$\int_0^{+\infty} \left(||e(t)||^2 + ||r(t)||^2\right)dt \leq \frac{V(0)}{\lambda_3} \tag{32}$$

from which it can easily be seen that $e(t)$ and $r(t)$ are square-integrable functions. Barbalat's Lemma [31] can then be used to obtain asymptotic operational space tracking and subtask control given in Eq. (24). □

Remark 5. At this point, we would like to point out that similar stability result, asymptotic end-effector and subtask tracking, can also be obtained using LaSalle's invariant set theorem [32].

6 Experimental Study

In order to demonstrate the performance of the proposed controller, an experimental study is conducted on a redundant robot manipulator. The 3DOF robot manipulator, as shown in Fig. 1, has an articulated structure with three links and three actuators and works on the plane. Direct drive actuators of E137576 Maxon Motors with the technical features of a nominal voltage of 24 VDC, a speed constant of 263 rpm/V, a nominal speed of 5530 rpm, and a nominal torque of 78.2 m N·m were used. The motors are driven by a Maxon Escon 36/2 DC 4-Q Servo-controller with a maximum power of 72 W. For an absolute angular measurement, AS5045 magnetic rotary encoders were used with a resolution of 4096 positions per revolution based on contactless magnetic sensor technology. The proposed control method is implemented on the computer and run on MATLAB SIMULINK by using a real time window target. The control inputs are transmitted to the motor drivers with analog signals, and encoder signals are received as quadrature counter inputs. The data transmission between the computer and the drivers is carried out with a Humusoft MF624 data acquisition board at the frequency of 1 kHz sampling rate.

Using Euler-Lagrange formulations, the generalized mass-inertia matrix and centripetal-Coriolis matrix can be represented as

$$M(\theta) = \begin{bmatrix} M_{11} & M_{12} & M_{13} \\ M_{12} & M_{22} & M_{23} \\ M_{13} & M_{23} & M_{33} \end{bmatrix} \tag{33}$$

$$V_m(\theta, \dot{\theta}) = \begin{bmatrix} V_{m11} & V_{m12} & V_{m13} \\ V_{m21} & V_{m22} & V_{m23} \\ V_{m31} & V_{m32} & V_{m33} \end{bmatrix} \tag{34}$$

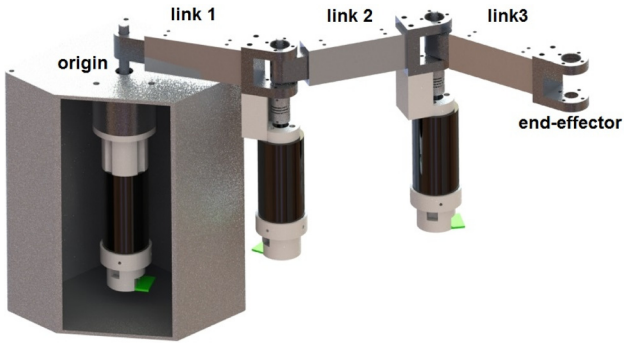

Fig. 1 3DOF planar redundant robot manipulator

where the entries of the mass-inertia matrix in Eq. (33) and the entries of the centripetal-Coriolis matrix in Eq. (34) (which are formed to satisfy Property 2) are given as follows:

$$\begin{aligned} M_{11} &= p_1 c_2 + p_2(c_3 + c_{23}) + p_3 & M_{22} &= p_2 c_3 + p_4 \\ M_{12} &= p_6 c_2 + p_2 c_3 + p_7 c_{23} + p_4 & M_{23} &= p_7 c_3 + p_5 \\ M_{13} &= p_7(c_3 + c_{23}) & M_{33} &= p_5 \end{aligned}$$

$$\begin{aligned} V_{m11} &= -(p_1 s_2 + p_2 s_{23})\dot{\theta}_2 - p_2(s_3 + s_{23})\dot{\theta}_3 \\ V_{m12} &= -(p_6 s_2 + p_7 s_{23})\dot{\theta}_2 - p_2(s_3 + s_{23})\dot{\theta}_3 \\ V_{m13} &= -p_7(s_3 + s_{23})\dot{\theta}_3 \\ V_{m21} &= (p_6 s_2 + p_7 s_{23})\dot{\theta}_1 \\ V_{m22} &= -p_2 s_3 \dot{\theta}_3 \\ V_{m23} &= -p_2 s_3 \dot{\theta}_1 - p_7 s_3 \dot{\theta}_3 \\ V_{m31} &= p_7(s_3 + s_{23})\dot{\theta}_1 \\ V_{m32} &= p_2 s_3 \dot{\theta}_1 + p_7 s_3 \dot{\theta}_2 \\ V_{m33} &= 0 \end{aligned}$$

where p_i ($i \in \{1, \ldots, 7\}$) denote the mass parameters (i.e., mass of the links, center of mass of each link, and link lengths) with unit kg m^2, s_i, c_i, $s_{i,j}$, $c_{i,j}$ represents $\sin(\theta_i)$, $\cos(\theta_i)$, $\sin(\theta_i + \theta_j)$, $\cos(\theta_i + \theta_j)$ ($i, j \in \{1, 2, 3\}$), respectively. The constant parameters are given as $p_1 = 0.0213$, $p_2 = 0.0029$, $p_3 = 0.0433$, $p_4 = 0.0177$, $p_5 = 0.0017$, $p_6 = 0.0106$, and $p_7 = 0.0015$ kg·m^2.

It should be noticed that the gravitational effects were not considered in this experiment since the manipulator is horizontally

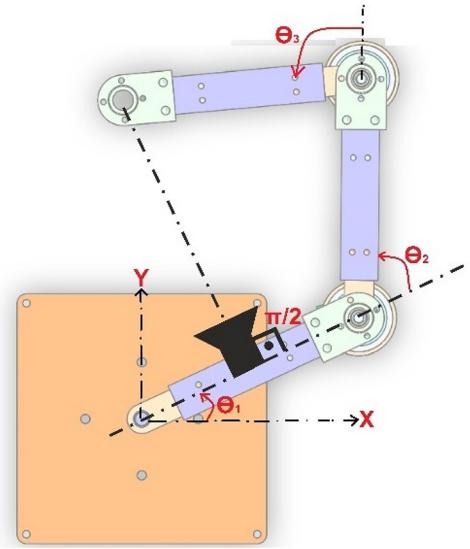

Fig. 2 Representation of the laser/camera tracer subtask

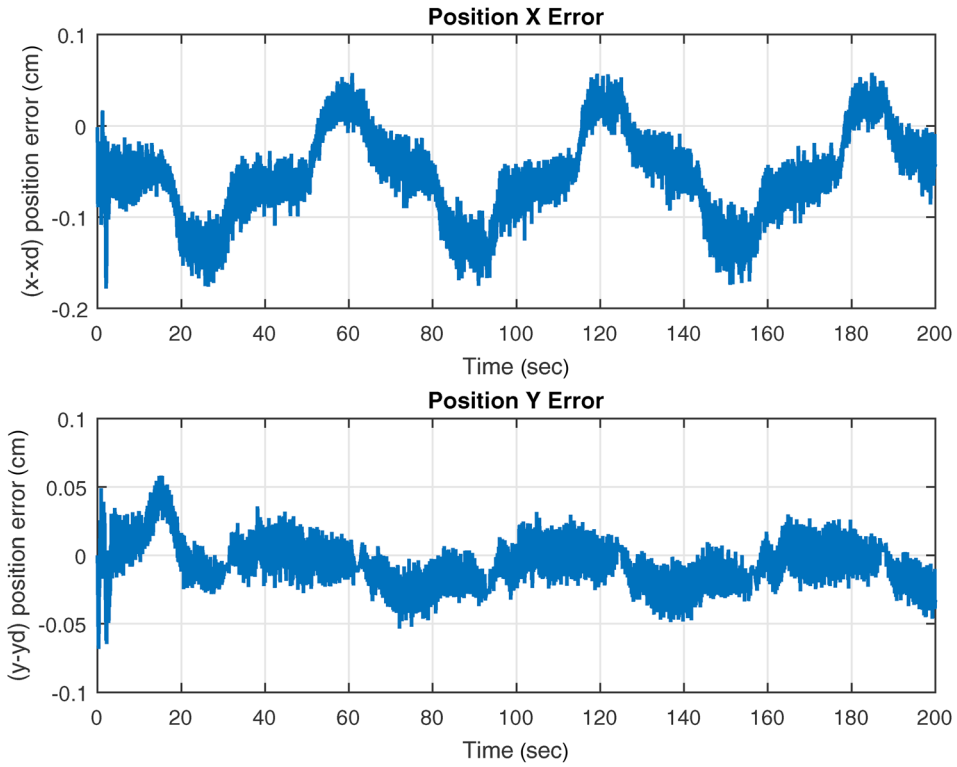

Fig. 3 Experiment: operational space tracking errors $e(t)$

moving on the plane. In addition, we also neglected the friction parameters since they do not have a significant effect.

Using Denavit–Hartenberg parameters, the end-effector position of the manipulator in the operational space can be obtained to have the following form:

$$x(t) = \begin{bmatrix} X(t) \\ Y(t) \end{bmatrix} = \begin{bmatrix} l_1 c_1 + l_2 c_{12} + l_3 c_{123} \\ l_1 s_1 + l_2 s_{12} + l_3 s_{123} \end{bmatrix} \tag{35}$$

where the link lengths are $l_1 = l_2 = l_3 = 0.127$ m and s_i, c_i, s_{ij}, c_{ij}, s_{ijk}, and c_{ijk} represent $\sin(\theta_i)$, $\cos(\theta_i)$, $\sin(\theta_i + \theta_j)$, $\cos(\theta_i + \theta_j)$,

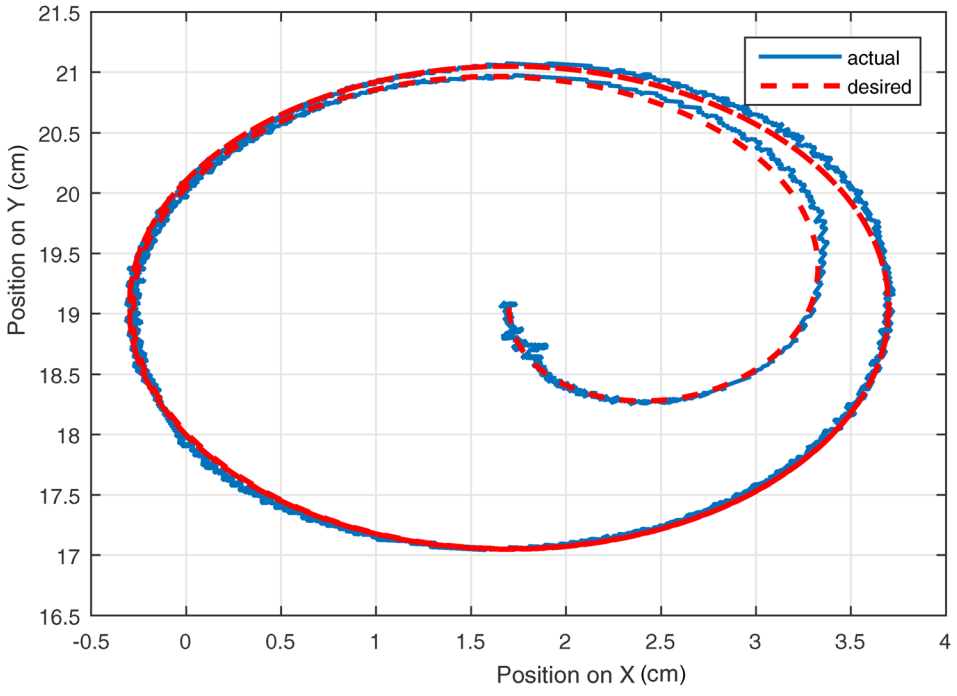

Fig. 4 Experiment: desired $x_d(t)$ and actual $x(t)$ operational space trajectories

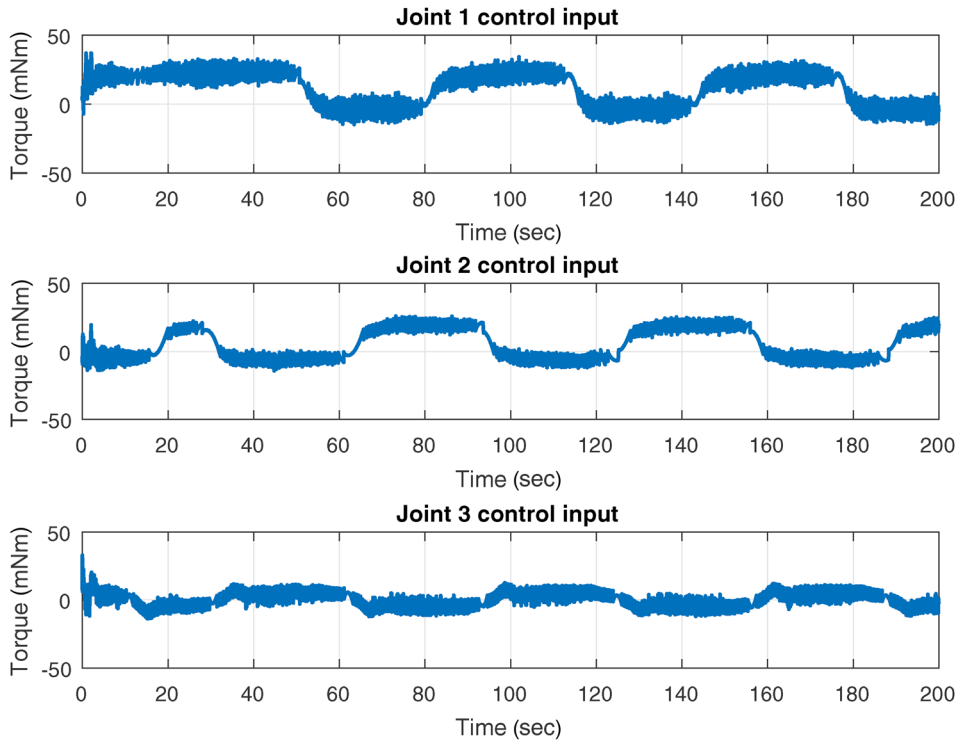

Fig. 5 Experiment: control input torques $\tau(t)$

$\sin(\theta_i + \theta_j + \theta_k)$, $\cos(\theta_i + \theta_j + \theta_k)$ $(i, j, k \in \{1, 2, 3\})$, respectively. Based on the above forward kinematic calculations, the manipulator Jacobian is obtained as

$$J = \begin{bmatrix} -l_1 s_1 - l_2 s_{12} - l_3 s_{123} & -l_2 s_{12} - l_3 s_{123} & -l_3 s_{123} \\ l_1 c_1 + l_2 c_{12} + l_3 c_{123} & l_2 c_{12} + l_3 c_{123} & l_3 c_{123} \end{bmatrix} \tag{36}$$

The manipulator was initialized to be at rest at the following joint position $\theta(0) = [0, \pi/2, \pi/3]^{\mathrm{T}}$ rad. The desired trajectory in the operational space was chosen as

$$x_d = \begin{bmatrix} X_d \\ Y_d \end{bmatrix} = \begin{bmatrix} 0.017 + 0.02 \sin(0.1t)\big(1 - \exp(-0.1t)\big) \\ 0.1905 - 0.02 \cos(0.1t)\big(1 - \exp(-0.1t)\big) \end{bmatrix} \tag{37}$$

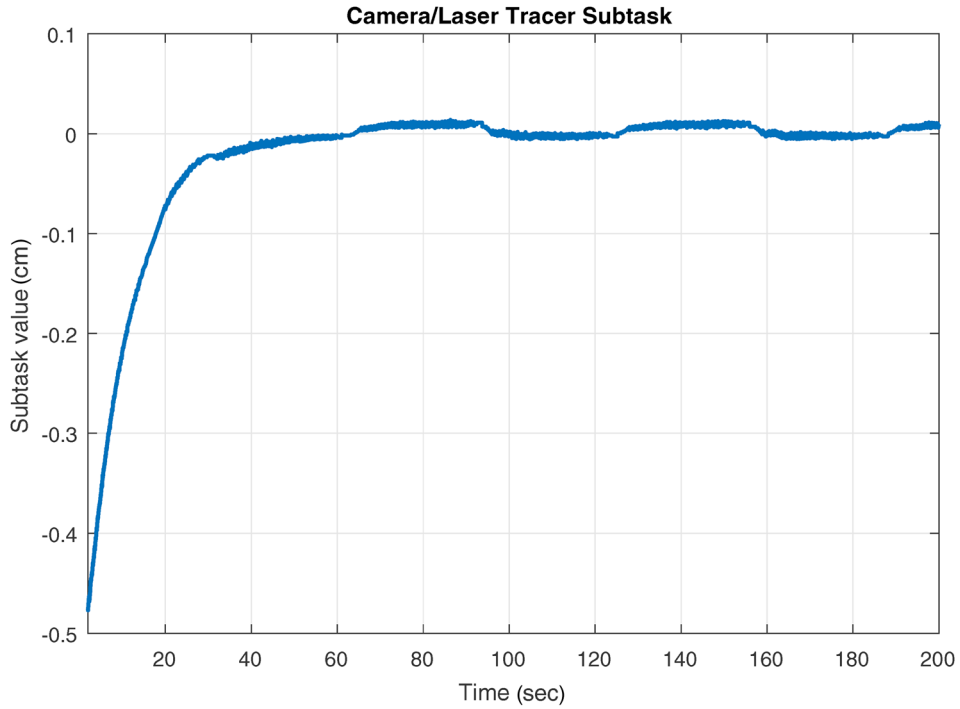

Fig. 6 Experiment: subtask function

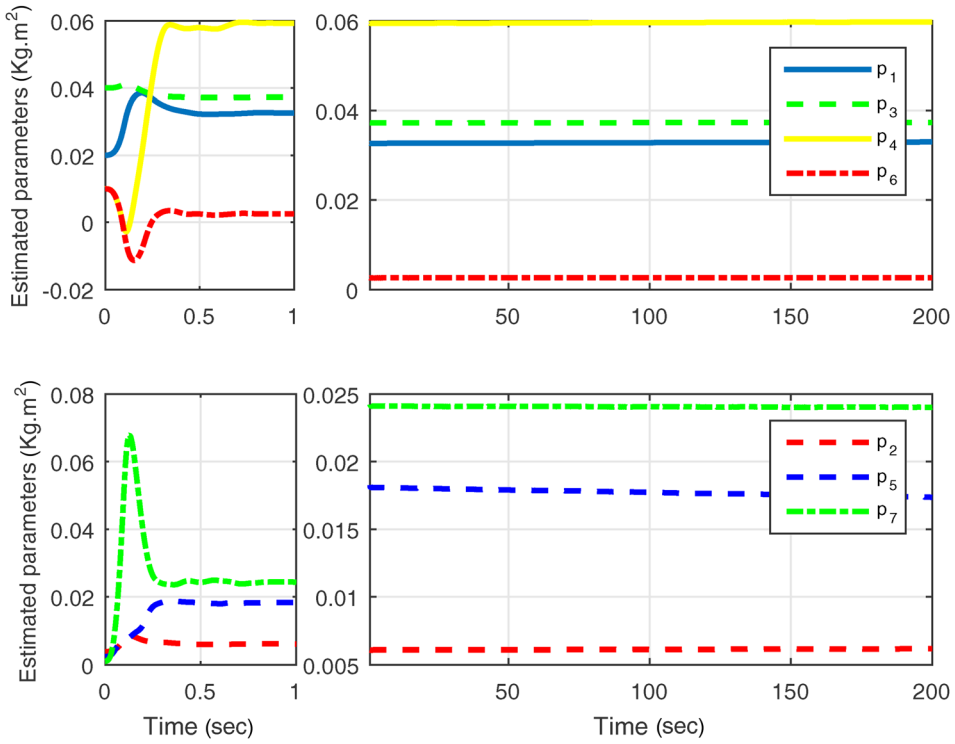

Fig. 7 Experiment: estimates of uncertain parameters $\hat{\phi}(t)$

In this experiment, we introduce a new subtask function (i.e., laser/camera tracer) that aims to allow a perpendicularly fixed laser beam or optic camera on the middle of the first joint which absolutely traces line of the sight of the end-effector of the manipulator. This novel subtask was motivated by the inspiring work [29] where two hyper redundant robot manipulators worked cooperatively to replace a section of a critical pipe in a nuclear jungle where one of them was only used to hold a vision system at its end-effector. As represented in Fig. 2, the subtask function can be trigonometrically written as follows:

$$y_s = \frac{l_1}{2} + l_2 c_2 + l_3 c_{23} \tag{38}$$

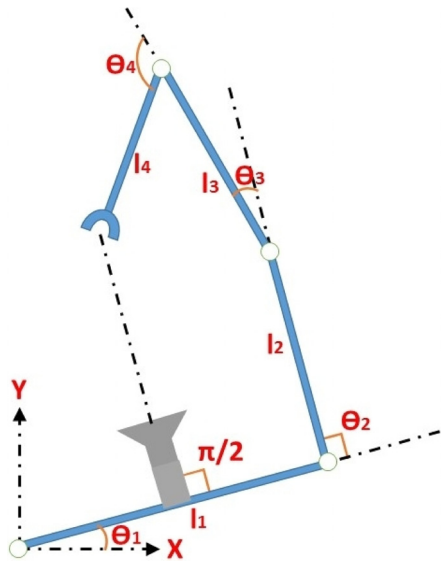

Fig. 8 4DOF planar redundant robot manipulator

According to the aim of the subtask function, the desired subtask is to force y_s to go to zero, and therefore, $y_d = 0$. It should be noted that this novel idea of the subtask function is not conducted with a real camera/laser equipment, but its mathematical model is performed in the experimental study.

After some trial and observing errors, we obtained the best results for the proposed controller of Eq. (20) with the following control and adaptation gains; $\alpha = 90 \times \text{diag}\{1.2, 1.1, 1\}$ and $K_r = 45 \times \text{diag}\{1.2, 1.1, 1\}$, $\Gamma = 10^{-4} \times I_7$. The initial values of the parameter update vector were chosen as $\hat{\phi}(0) = 10^{-3} \times [20, 2, 40, 10, 1, 10, 1]^{\mathrm{T}}$.

The operational space tracking errors are presented in Fig. 3. It is observed that errors on X and Y coordinates of the end-effector are less than 1 mm, which is an acceptable value when compared to the operational space of the end-effector. Figure 4 illustrates the actual and desired operational space trajectories. From Figs. 3 and 4, it is observed that the end-effector position converged to the desired task position. Figure 5 shows the applied torques to the three joints. As it is expected, the control input torque values of each three joints are quite lower than the maximum continuous torque of 78.2 m N·m. From the result of the subtask objective shown in Fig. 6, it is observed that the subtask function value went to the desired subtask value and satisfied the subtask objective. Finally, Fig. 7 presents the estimates of uncertain parameters. As observed from Fig. 7, the estimated values of the uncertain parameters approximately converge to some values in finite time, which means that our adaptive update rule worked well. It should be noted that different initial values were also tried, and similar good results were obtained during the experimental study.

7 Simulation Study

In this section, a simulation study results is presented to show the validity of the proposed controller with multiple subtask objectives. For this numerical study, a 4DOF planar robot manipulator, as shown in Fig. 8, is simulated on MATLAB/SIMULINK with a data rate of 1 kHz. As the authors obtained in Refs. [33] and [34], the kinematic and dynamic models of 4DOF planar robot

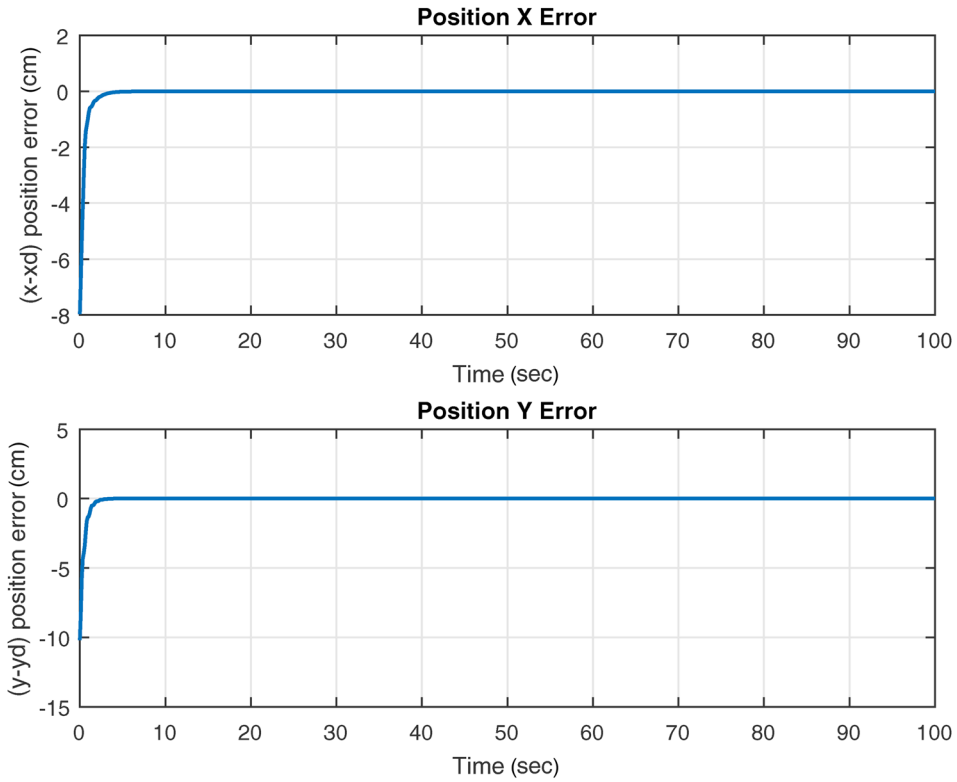

Fig. 9 Simulation: operational space tracking errors $e(t)$

manipulator are modeled. The end-effector position of the manipulator in the operational space can be written as

$$x(t) = \begin{bmatrix} X(t) \\ Y(t) \end{bmatrix} = \begin{bmatrix} l_1 c_1 + l_2 c_{12} + l_3 c_{123} + l_4 c_{1234} \\ l_1 s_1 + l_2 s_{12} + l_3 s_{123} + l_4 s_{1234} \end{bmatrix} \tag{39}$$

where the link lengths are $l_1 = 0.6\,\text{m}, l_2 = l_3 = 0.4\text{m}, l_4 = 0.3\,\text{m}$ and s_{1234} and c_{1234} represent $\sin(\theta_{1234})$ and $\cos(\theta_{1234})$, respectively.

Initial joint positions of the manipulator were chosen as $\theta(0) = [\pi/10, 2\pi/5, \pi/10, \pi/4]^{\text{T}}$ rad. The desired operational space trajectory was selected as follows:

$$x_d = \begin{bmatrix} X_d \\ Y_d \end{bmatrix} = \begin{bmatrix} 0.1 + 0.05\cos(0.1t)\big(1 - \exp(-0.1t)\big) \\ 1.0 + 0.05\sin(0.1t)\big(1 - \exp(-0.1t)\big) \end{bmatrix} \tag{40}$$

Since the 4DOF planar robot manipulator has two redundant DOF, two different subtask functions can be introduced in this

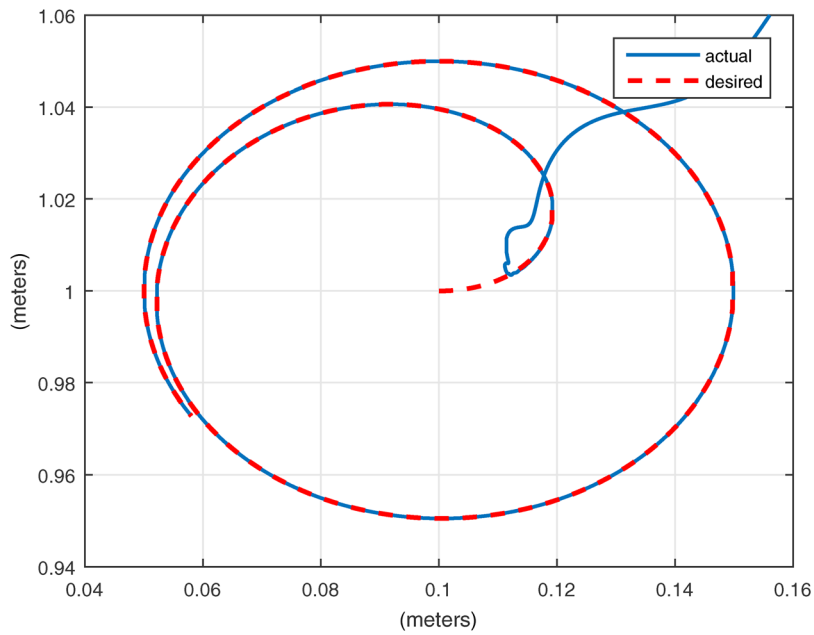

Fig. 10 Simulation: desired $x_d(t)$ and actual $x(t)$ operational space trajectories

simulation study. The first subtask function with the same objective (laser/camera tracer) in Sec. 6 can be trigonometrically written as follows:

$$y_{s1} = \frac{l_1}{2} + l_2\cos(\theta_2) + l_3\cos(\theta_2+\theta_3) + l_4\cos(\theta_2+\theta_3+\theta_4) \tag{41}$$

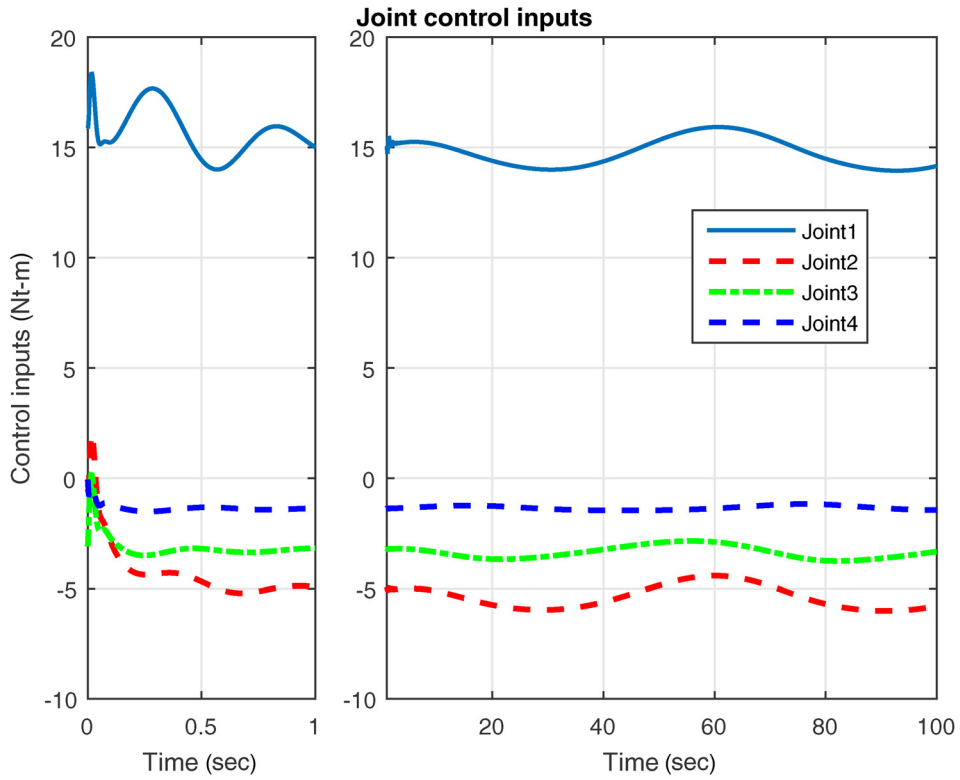

Fig. 11 Simulation: control input torques $\tau(t)$

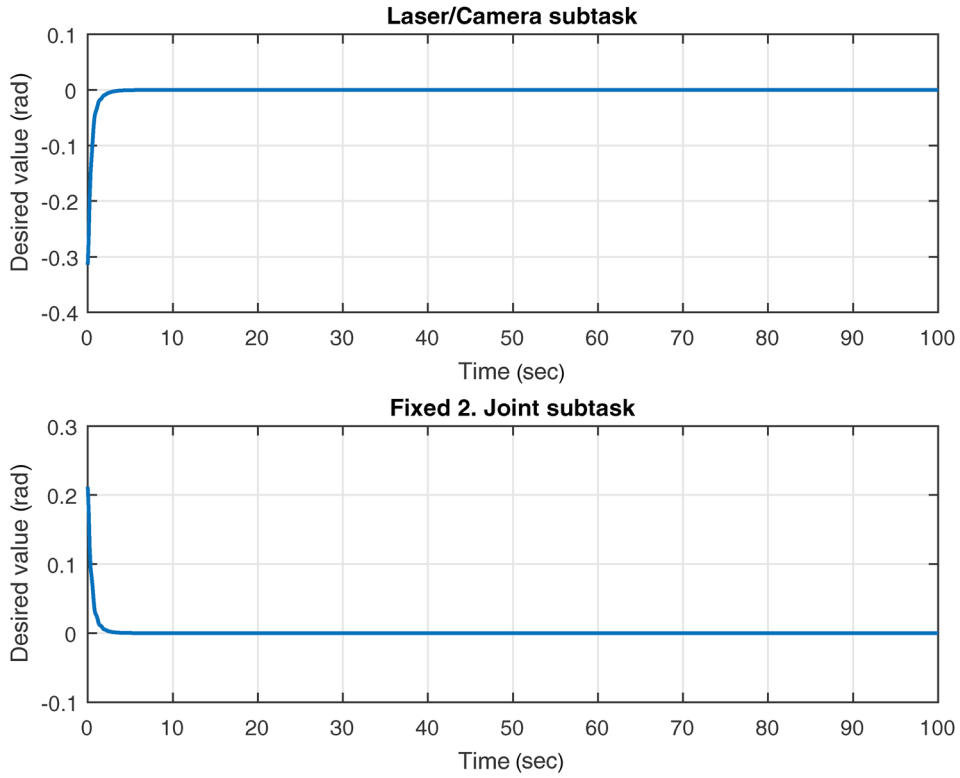

Fig. 12 Simulation: subtask functions $y_{s1}(\theta)$ and $y_{s2}(\theta)$

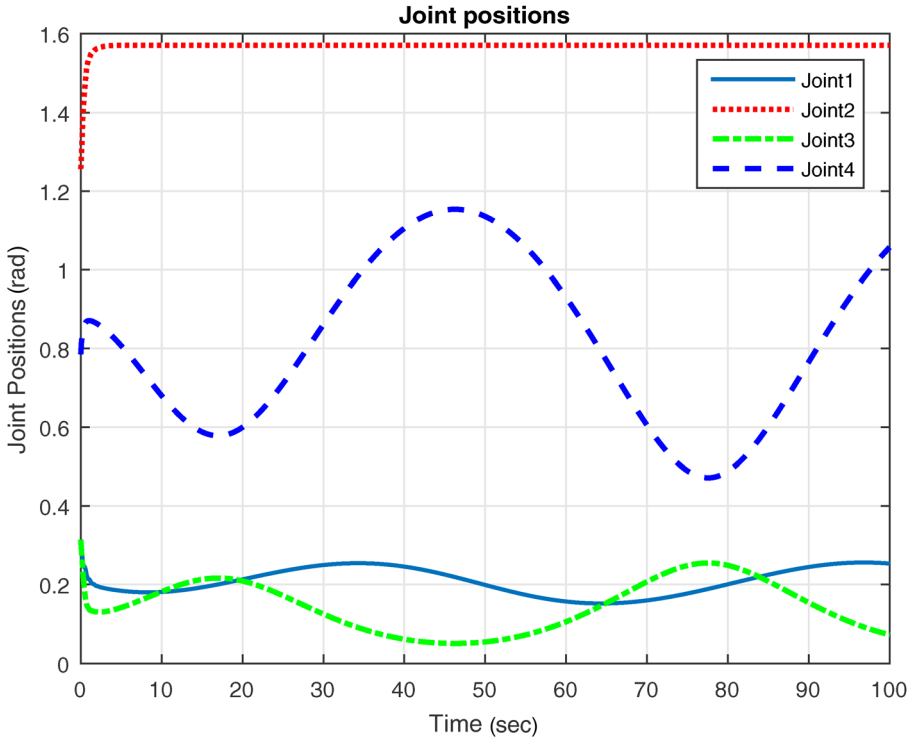

Fig. 13 Simulation: four joint positions

The second subtask function might be related to the first subtask function to be more realistic in industrial applications. It is noticed that the relationship between the first subtask objective and the second or the rest subtask objectives is not mandatory for the proposed method. As shown in an example of Fig. 8, for the alignment of the laser/camera setup on the middle of the first link, the second link might be used to handle the setup as perpendicularly. Therefore, the second subtask function aims to force a joint to go to a desired angle and is selected as follows:

$$y_{s2} = \theta_2 - \pi/2 \tag{42}$$

According to the aim of the subtask functions, both desired subtasks are to force y_{s1} and y_{s2} to go to zero, therefore $y_{d1} = y_{d2} = 0$. The adaptive controller of Eq. (20) was obtained

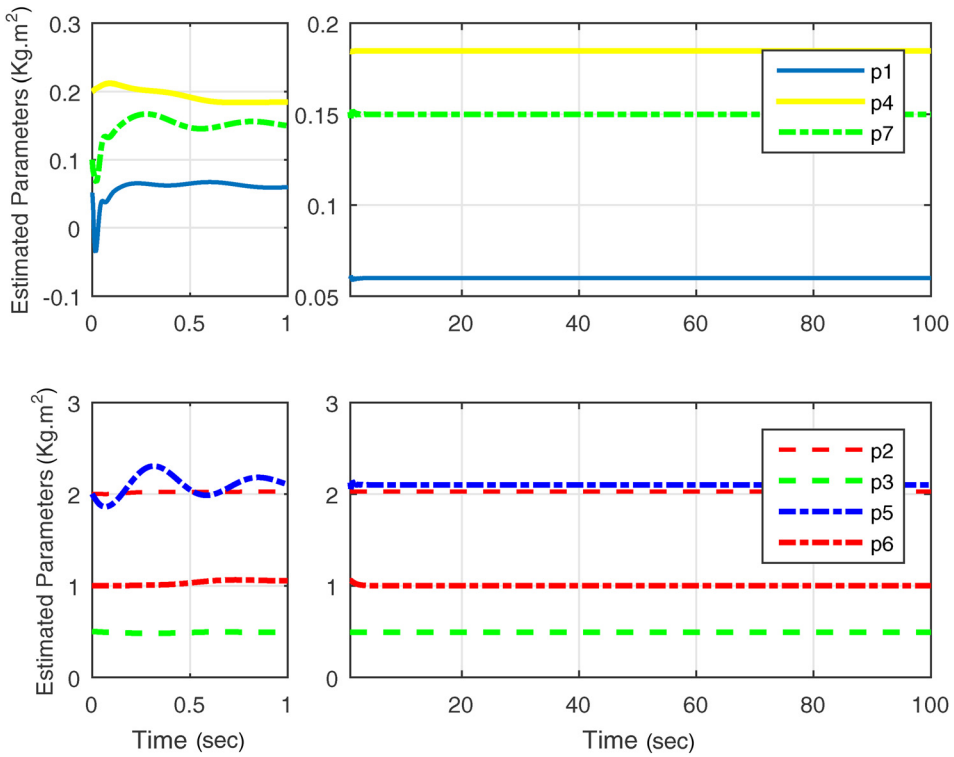

Fig. 14 Simulation: estimates of uncertain parameters $\hat{\phi}(t)$

with the following control and adaptation gains; $\alpha = K_r = 2 \times I_{4\times}$, $\Gamma = I_7$. The initial values of the parameter update vector were chosen as $\hat{\phi}(0) = [0.05, 2, 0.5, 0.2, 2, 1, 0.1]^{\mathrm{T}}$.

As illustrated in Fig. 9, the operational space tracking errors converge to zero on X and Y coordinates of the end-effector. Figure 10 presents the desired and actual operational space trajectories. From Figs. 9 and 10, it is observed that the end-effector position converges to the desired end-effector position. As shown in Fig. 11, control input torques applied to the four joints are relatively smooth. Figure 12 shows the two subtask functions. It is clear that both subtask functions went to the desired subtask values and satisfied the multiple subtask objectives. From the angle positions of four joints in Fig. 13, it is seen that the second joint is forced to go to $\pi/2$ rad, which is the second subtask objective. Figure 14 shows the estimates of uncertain parameters.

8 Conclusions

The main focus of this study is to design an extended operational space controller formulation with multiple subtask objectives for kinematically redundant robot manipulators with uncertain dynamical parameters. The aim is to make the extended Jacobian to be full-rank by extending the operational space controller with subtask objectives as an amount of the redundant DOFs. To deal with uncertain dynamics, a standard adaptive control method has been designed. The stability of the overall system and convergence of the operational space tracking and subtask objectives are ensured via Lyapunov based arguments.

Experimental studies on the 3DOF kinematically redundant robot manipulator were conducted using the proposed controller with a subtask objective. In the novel subtask objective, the redundant robot manipulator was considered as being equipped with a camera or laser on one of the links that trace the end-effector of the manipulator while performing the main end-effector tracking objective. To illustrate the performance of the proposed method for the multiple subtask objectives, simulation studies were performed on the model of 4DOF kinematically redundant robot manipulator.

The proposed extended operational space controller is novel when compared to the existing literature on control of kinematically redundant robot manipulators. When compared to the augmented based Jacobian methods in the literature [22]–[28], our proposed method achieves asymptotic subtask tracking and asymptotic operational space tracking while the adaptive controller of Ref. [25] ensures globally ultimately extended operational space tracking. As opposed by the operational space controller along with the pseudo-inverse of Jacobian-based null-space controller in Refs. [11,12], and [16], our extended Jacobian-based controller (20) allows us to carry out a combined stability analysis for both operational space tracking and subtask objectives without requiring to design an external null-space controller. In addition, the other advantage of the proposed controller (20) is able to apply to hyper redundant robot manipulators without requiring a separate stability analysis for multiple subtask objectives while still ensuring the operational space control objective.

Funding Data

- The Scientific and Technological Research Council of Turkey (Grant No. 113E147; Funder ID: 10.13039/501100004410).

References

[1] Conkur, E. S., and Buckingham, R., 1997, "Clarifying the Definition of Redundancy as Used in Robotics," Robotica, **15**(5), pp. 583–586.
[2] Siciliano, B., 1990, "Kinematic Control of Redundant Robot Manipulators: A Tutorial," J. Intell. Rob. Syst., **3**(3), pp. 201–212.
[3] Nakamura, Y., 1991, *Advanced Robotics Redundancy and Optimization*, Addison-Wesley, Reading, MA.
[4] Siciliano, B., and Khatib, O., 2008, *Springer Handbook of Robotics*, Springer, Secaucus, NJ.
[5] Khatib, O., 1983, "Dynamic Control of Manipulators in Operational Space," IFTOMM Congress on the Theory of Machines and Mechanisms, New Delhi, India, pp. 1–10.
[6] Hsu, P., Hauser, J., and Sastry, S., 1989, "Dynamic Control of Redundant Manipulators," J. Rob. Syst., **6**(2), pp. 133–148.
[7] Ott, C., Dietrich, A., and Albu-Schffer, A., 2015, "Prioritized Multi-Task Compliance Control of Redundant Manipulators," Automatica, **53**, pp. 416–423.
[8] Luo, S., and Ahmad, S., 1997, "Adaptive Control of Kinematically Redundant Robots," IMA J. Math. Control Inf., **14**, pp. 225–253.
[9] Zergeroglu, E., Dawson, D., Walker, I. D., and Behal, A., 2000, "Nonlinear Tracking Control of Kinematically Redundant Robot Manipulators," American Control Conference (ACC), Chicago, IL, June 28–30, pp. 2513–2517.
[10] Zergeroglu, E., Dawson, D. M., Walker, I. D., and Setlur, P., 2004, "Nonlinear Tracking Control of Kinematically Redundant Robot Manipulators," IEEE/ASME Trans. Mechatronics, **9**(1), pp. 129–132.
[11] Tatlicioglu, E., McIntyre, M. L., Dawson, D. M., and Walker, I. D., 2005, "Adaptive Nonlinear Tracking Control of Kinematically Redundant Robot Manipulators With Sub-Task Extensions," IEEE Conference on Decision and Control, Seville, Spain, Dec. 15, pp. 4373–4378.
[12] Tatlicioglu, E., McIntyre, M. L., Dawson, D. M., and Walker, I. D., 2008, "Adaptive Non-Linear Tracking Control of Kinematically Redundant Robot Manipulators," Int. J. Rob. Autom., **23**(2), pp. 98–105.
[13] Tatlicioglu, E., Braganza, D., Burg, T. C., and Dawson, D. M., 2008, "Adaptive Control of Redundant Robot Manipulators With Sub-Task Extensions," American Control Conference, Seattle, WA, pp. 856–861.
[14] Tatlicioglu, E., Braganza, D., Burg, T. C., and Dawson, D. M., 2009, "Adaptive Control of Redundant Robot Manipulators With Sub-Task Objectives," Robotica, **27**(6), pp. 873–881.
[15] Tee, K. P., and Yan, R., 2011, "Adaptive Operational Space Control of Redundant Robot Manipulators," American Control Conference, San Francisco, CA, June 29–July 1, pp. 1742–1747.
[16] Cetin, K., Tatlicioglu, E., and Zergeroglu, E., 2016, "On Null–Space Control of Kinematically Redundant Robot Manipulators," European Control Conference, Aalborg, Denmark, June 29–July 1, pp. 678–683.
[17] Braganza, D., McIntyre, M. L., Dawson, D. M., and Walker, I. D., 2006, "Whole Arm Grasping Control for Redundant Robot Manipulators," American Control Conference, Minneapolis, MN, June 14–16, pp. 3194–3199.
[18] Zergeroglu, E., Sahin, H. T., Ozbay, U., and Tektas, U. A., 2006, "Robust Tracking Control of Kinematically Redundant Robot Manipulators Subject to Multiple Self-Motion Criteria," IEEE International Conference on Control Application, Munich, Germany, Oct. 4–6, pp. 2860–2865.
[19] Sahin, H. T., Ozbay, U., and Zergeroglu, E., 2006, "Quaternion Based Robust Tracking Control of Kinematically Redundant Manipulators Subject to Multiple Self-Motion Criteria," IEEE International Conference on Decision and Control, San Diego, CA, Dec. 13–15, pp. 6462–6467.
[20] Kapadia, A., Tatlicioglu, E., and Dawson, D. M., 2008, "Set-Point Navigation of a Redundant Robot in Uncertain Environments Using Finite Range Sensors," IEEE International Conference on Decision and Control, Cancun, Mexico, Dec. 9–11, pp. 4596–4601.
[21] Ren, Y., Zhou, Y., Liu, Y., Gu, Y., Jin, M., and Liu, H., 2017, "Robust Adaptive Multi-Task Tracking Control of Redundant Manipulators With Dynamic and Kinematic Uncertainties and Unknown Disturbances," Adv. Rob., **31**(9), pp. 482–495.
[22] Baillieul, J., 1985, "Kinematic Programming Alternatives for Redundant Manipulators," IEEE International Conference on Robotics and Automation, St. Louis, MO, Mar. 25–28, pp. 722–728.
[23] Seraji, H., 1989, "Configuration Control of Redundant Manipulators: Theory and Implementation," IEEE Trans. Rob. Autom., **5**(4), pp. 472–490.
[24] Peng, Z., and Adachi, N., 1993, "Compliant Motion Control of Kinematically Redundant Manipulators," IEEE Trans. Rob. Autom., **9**(6), pp. 831–837.
[25] Colbaugh, R., and Glass, K., 1995, "Robust Adaptive Control of Redundant Manipulators," J. Intell. Rob. Syst., **14**(1), pp. 68–88.
[26] Benzaoui, M., Chekireb, H., and Tadjine, M., 2010, "Redundant Robot Manipulator Control With Obstacle Avoidance Using Extended Jacobian Method," 18th Mediterranean Conference on Control Automation (MED), Marrakech, Morocco, June 23–25, pp. 371–376.
[27] Simas, H., Dias, A., and Martins, D., 2011, "Extended Jacobian for Redundant Robots Obtained From the Kinematics Constraints," 21th International Congress of Mechanical Engineering, Natal, Brazil, pp. 1005–1014.
[28] Karpinska, J., and Tchon, K., 2012, "Performance-Oriented Design of Inverse Kinematics Algorithms: Extended Jacobian Approximation of the Jacobian Pseudo-Inverse," ASME. J. Mech. Rob., **4**(2), p. 021008.
[29] Buckingham, R., and Graham, A., 2005, "Snaking Around in a Nuclear Jungle," Ind. Rob.: An Int. J., **32**(2), pp. 120–127.
[30] Lewis, F., Dawson, D., and Abdallah, C., 2004, *Robot Manipulator Control: Theory and Practice*, Marcel Dekker, New York.
[31] Krstic, M., Kanellakopoulos, I., and Kokotovic, P., 1995, *Nonlinear and Adaptive Control Design*, Wiley, New York.
[32] Khalil, H., 2002, *Nonlinear Systems*, Prentice Hall PTR, Upper Saddle River, NJ.
[33] Kircanski, M., 1996, "Kinematic Isotropy and Optimal Kinematic Design of Planar Manipulators and a 3-DOF Spatial Manipulator," Int. J. Rob. Res., **15**(1), pp. 61–77.
[34] Mandava, R. K., and Vundavalli, P. R., 2015, "Design of Pid Controllers for 4-DOF Planar and Spatial Manipulators," International Conference on Robotics, Automation, Control and Embedded Systems (RACE), Chennai, India, Feb. 18–20, pp. 1–6.